High speed loading of concrete constructions with transformation of eroded mass into the SPH

Jiří Kala, and Martin Hušek

***Abstract*—**The paper describes some negative aspects of high speed loading simulations by using the finite elements method. A simple terminal ballistics experiment illustrates the issue. It consists in a collision of a high speed flying fragment with a concrete target. Penetration and spalling of the concrete target surface are considered as main characteristics of the failure. A large elements deformation in the simulations causes numerical problems such as elements locking, negative volumes formation and increased computational time. These negative simulations aspects can be removed by using some numerical tools such as elements erosion and eroded mass transformation into smoothed particle hydrodynamics. The both numerical tools are explained and their connection with a material model physical nature as well as their application in the simulation are described afterwards. The results show the functionality of these tools in the end of the paper.

***Keywords*—**High-speed impact, nonlinear constitutive model, numerical erosion, smoothed particle hydrodynamics.

I. Introduction

IN the modern world, the use of concrete as a construction material is very popular. As a result, variants of material models are being developed which can deal with the issues that arise as well as possible [1]–[4].

In the case of high-speed processes which take place at the millisecond level, there are different requirements for material models [5]–[9]. Consideration of the loading rate is often of key importance for the attainment of results which correspond to reality [10], [11]. Material models have thus become very complex and often need a great quantity of input data so that the calculation can be carried out. As a result, they are becoming user unfriendly due to the fact that long series of experimental measurements are needed to obtain input data before the simulation itself can be carried out. On the other hand, material models which contain algorithms generating input data on the basis of very little information are becoming highly popular. In the systems which are most commonly used for the simulation of high-speed nonlinear dynamic events, such as LS-DYNA [1] or AUTODYN [12], material models are available which enable such algorithms to be employed.

A very popular material model for high speed impact simulations is the HJC (Holmquist-Johnson-Cook) model [1], [13], [14] – one of a group of nonlinear material models of concrete that enable the effect of strain rate on the state of stress to be taken into account. It is intended for the simulation of processes taking place over short intervals of time. The model is primarily intended for the modelling of concrete structures subject to great deformation, high strain rate and high compression.

In many studies concerning the issues raised by the penetration, fragmentation and perforation of concrete structures [15]–[19], the numerical erosion of elements is not handled at all, or is only dealt with to a very limited degree, even though it is always used in simulations. The sensitivity of test results is strongly dependent [12] on the choice of erosion criterion [20]. Even though correlative relationships between the energy of the projectile and the parameters of the concrete structure can be used in several cases [21], [22] and thus the results of a simulation or experiment can be predicted, the estimate will always be very rough and it will only distinguish the degree of damage – penetration or perforation. It is therefore undeniably advantageous to use numerical simulations. In order that the results of numerical simulations are usable and can serve other purposes, they have to be supported by an experiment [23]–[27] or simulation techniques have to be used which will suppress false dependence, such as the aforementioned problem with dependence on the choice of numerical erosion.

After the execution of an experiment, the same results can easily be achieved by numerical simulations by simply setting [28], [29] (for example) the criteria for the erosion of elements to a suitable value [30], [31]. However, if the simulation was conducted before the experiment, and the finite element method (FEM) simulation was used because of its advantages, other extensions would have to be used which would suppress artificial numerical dependences of (for example) the mesh sensitivity or element erosion type.

Even though good agreement with experiments can be achieved by using a different hydrocode than FEM for the simulation of penetration and perforation [32], [33], and by doing so avoid the appearance of negative properties due to

This outcome has been achieved with the financial support of project GACR 14-25320S "Aspects of the use of complex nonlinear material models" provided by the Czech Science Foundation.

J. Kala is with the Faculty of Civil Engineering, Institute of Structural Mechanics, Brno University of Technology, Czech Republic (e-mail: kala.j@fce.vutbr.cz).

M. Hušek is with the Faculty of Civil Engineering, Institute of Structural Mechanics, Brno University of Technology, Czech Republic (e-mail: husek.m@fce.vutbr.cz).

false dependence on the final element mesh, other problems can arise in many cases, one example being mesh-free methods [34]–[36]. However, if several computational methods could be effectively combined, the strong points of both of them could be utilized.

II. The Erosion Problem

The element erosion function, while not a material property or physics-based phenomenon, provides a useful means of simulating the spalling of concrete and provides a more realistic graphical representation of actual impact events. Erosion is characterized by the physical separation of the eroded solid element from the rest of the mesh [37]. Though element removal (erosion) associated with total element failure has the appearance of physical material erosion, it is, in fact, a numerical technique used to permit the extension of the computation. Without numerical erosion, severely crushed elements in Lagrangian calculations would drive to a very small time step, resulting in the use of many computational cycles with a negligible advance in the simulation time. Moreover, Lagrangian elements which have become very distorted have a tendency to "lock up," thereby inducing unrealistic distortions in the computational mesh [38]. The erosion function allows the removal of such Lagrangian cells from the calculation if a predefined criterion is reached. When a cell is removed from the calculation process, the mass within the cell can either be discarded or distributed to the corner nodes of the cell. If the mass is retained, the conservation and spatial continuity of inertia are maintained.

However, the compressive strength and internal energy of the material within the cell are lost whether the mass is retained or not. Even though the filtering out of unsuitable (unneeded) elements is more a matter for numerical simulations, it can be connected (to a certain degree) with the physical matter of the material model.

A. Residual Compressive Strength with SPH

The moment at which an element of the Lagrangian mesh erodes is in conflict with what happens in real life, however. In reality, the material does not cease to exist but is only crushed and flakes off – see Fig. 1.

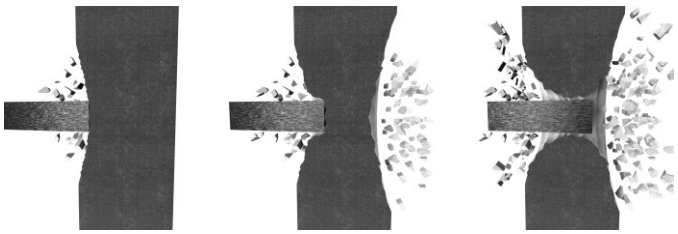

Fig. 1. Schematic diagrams showing from the left: penetration, scabbing and perforation of concrete slabs struck by "hard" missiles.

Even though one cannot speak about the strength of the material as such, the particles and wedge-shaped fragments that fly off can create secondary or residual strength. In order to better approximate reality, it is advantageous to maintain the presence of even such particles in the simulation. This can be done via the transformation of eroded elements into SPH (Smoothed Particle Hydrodynamics) particles. Subsequently, these freely moving particles with the characteristics of the original materials will interact with the rest of the computational model and thus better reflect reality.

III. The HJC Material Model

Under shock wave compression, plastic deformation and crack-induced damage should be taken into account in the modelling of concrete behaviour. A constitutive law combining pressure-dependent plastic hardening, damage-softening and the strain rate effect, especially suited for the prediction of concrete response under dynamic loading such as blasts and impacts [39], was developed by Holmquist *et al.* [13]. In this constitutive law the normalised equivalent stress is defined as

$$\sigma^* = [A(1-D) + BP^{*N}][1 + C\ln(\dot{\varepsilon}^*)] \leq S_{max} \tag{1}$$

where $\sigma^* = \sigma/f_c'$ and $P^* = P/f_c'$ are the normalised equivalent stress and pressure, with σ and f_c' being the actual equivalent stress and the quasi-static uniaxial compressive strength, respectively. Scalar damage D is a value from 0 to 1 that describes the accumulation of damage as a percentage of the full cohesive strength that the material possesses. When $D = 0$, the material is undamaged and exhibits its full strength, but at $D = 1$ the material is fully damaged and retains the least confined shear strength. $\dot{\varepsilon}^* = \dot{\varepsilon}/\dot{\varepsilon}_0$ is the dimensionless strain rate, where $\dot{\varepsilon}$ and $\dot{\varepsilon}_0$ are the actual and reference strain rates, respectively. The material constants are A, B, C, N and S_{max}, where A is the normalized cohesive strength, B is the normalized pressure hardening coefficient, C is the strain rate coefficient, N is the pressure hardening exponent and S_{max} is the normalized maximum strength that can be developed.

The model accumulates damage from both equivalent plastic strain $\Delta\varepsilon_p$ and plastic volumetric strain $\Delta\mu_p$. The compression damage is expressed as

$$D = \sum \frac{\Delta\varepsilon_p + \Delta\mu_p}{D_1(P^* + T^*)^{D_2}} \tag{2}$$

where D_1 and D_2 are material constants; $T^* = T/f_c'$ is the normalised maximum tensile hydrostatic pressure that the material can withstand, and T is the maximum tensile hydrostatic pressure.

The equation of state (EOS linear elastic region, transition region and compact region) is expressed as follows [13], [14] for loading

$$P = \begin{cases} K_{elastic}\mu & 0 \leq \mu \leq \mu_{crush} \\ P_{crush} + \dfrac{(P_{lock} - P_{crush})(\mu - \mu_{crush})}{(\mu_{lock} - \mu_{crush})} & \mu_{crush} < \mu \leq \mu_{lock} \\ K_1\bar{\mu} + K_2\bar{\mu}^2 + K_3\bar{\mu}^3 & \mu > \mu_{lock} \end{cases} \tag{3}$$

where $\mu = \rho/\rho_0 - 1$ is the standard volumetric strain; $K_{elastic} = P_{crush}/\mu_{crush}$ is the elastic bulk modulus; ρ and ρ_0 are the current and initial densities, respectively; μ_{crush} and μ_{lock} are the crushing and locking volumetric strains, respectively; P_{crush} and P_{lock} are the crushing and locking pressures; and K_1, K_2 and K_3 are pressure constants – see Fig. 2. The modified volumetric strain $\bar{\mu}$ is defined as

$$\bar{\mu} = (\mu - \mu_{lock})/(1 + \mu_{lock}) \quad (4)$$

The tensile pressure is limited to $T(1 - D)$ during numerical calculations.

A. Implementation of Erosion

The HJC material model offers the implementation of element erosion on the basis of the size of the damage strength, D_s. The damage strength, D_s, is defined in compression when $P^* > 0$ as

$$D_s = f_c' \min[S_{max}; A(1 - D) + BP^{*N}]\,[1 + C\ln(\dot{\varepsilon}^*)] \quad (5)$$

or in tension if $P^* < 0$, as

$$D_s = f_c'\ \max\left[0; A(1 - D) - A\left(\frac{P^*}{T}\right)\right][1 + C\ln(\dot{\varepsilon}^*)] \quad (6)$$

The element erodes at the moment when its damage strength D_s falls below 0. From the physical point of view the implementation of such an algorithm is justified [1].

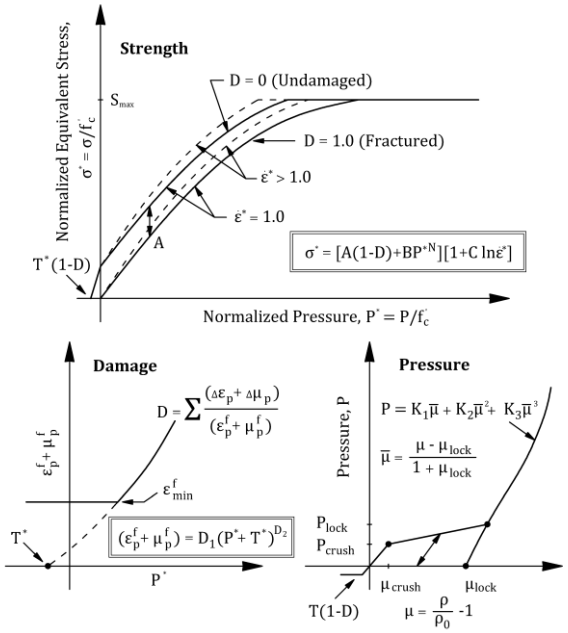

Fig. 2. Graphical representation of the HJC material model [13].

B. Transformation of Eroded Elements

If the above-mentioned problem with eroded matter and its dissipation were not solved, in extreme cases results might be gained which appear not to make sense. An example of this can be found in Fig. 3, where a concrete specimen impacts a rigid base at high speed. At the moment when the specimen comes into contact with the base, it starts to be crushed. The kinetic energy of the specimen transforms into plastic deformations of its body, and the specimen thus starts to slow down. Fig. 3 compares the progression of the impact of the specimen when its numerical description does not enable erosion of the elements (on the left), and when it does enable such erosion (in the middle). It is obvious that the results are significantly different in the final stage. The top surface of the specimen with element erosion almost falls onto the base, while the top part of the specimen without such erosion remains at half its original height.

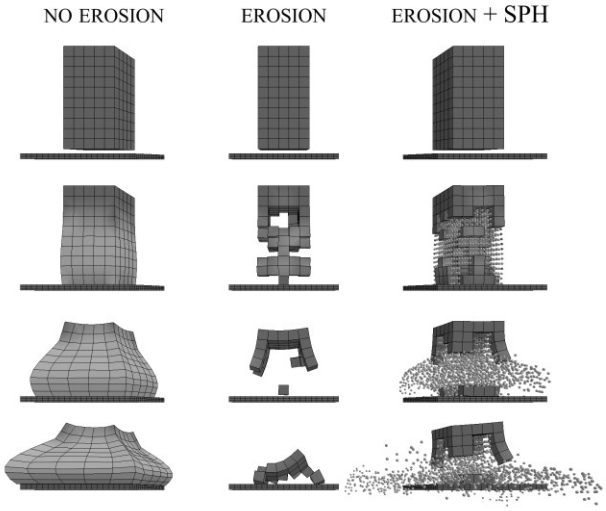

Fig. 3. Phases of the impact of a concrete specimen. From the left: model variant with no erosion, with erosion and with erosion and adaptive transformations into SPH.

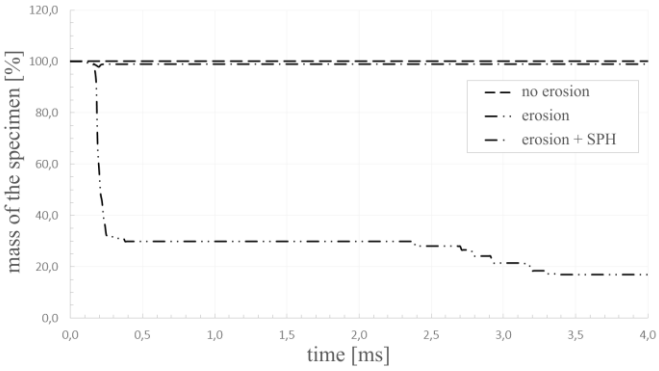

Fig. 4. Mass of the specimen through the simulation.

Even though the assumption was introduced that the only elements which will be eliminated from the calculation are those that would be in the stage of full failure from the perspective of the material model, and therefore would not influence the further course of the simulation significantly, it is obvious from the results that such a simple implementation of numerical erosion is inadequate, even if it is linked to the material model.

The third variant of the sample in Fig. 3 (on the right) includes the adaptive transformation of eroded elements into SPH particles. These particles have assumed the material properties of the eroded elements, and their weight and speed,

but also their stress state, etc. More information on SPH can be found in [40].

It can be concluded from the results that the described residual strength appears thanks to SPH particles. This strength is represented by the interaction of SPH particles with the rest of the numerical model and simultaneously with one another. The variant of the model with SPH particles then corresponds well with the original model where erosion was not included. Mass of the specimen through the simulation is shown in Fig. 4.

IV. The Experiment and Simulation

In 2002 J. Buchar *et al.* [41] performed an experiment with projectiles defined by the NATO STANAG 2920 standard, which they shot at speeds of 300 – 1400 ms^{-1} into concrete targets with the dimensions 0.1 x 0.1 x 0.1 m and a strength in compression of 43.1 MPa. The mass of the projectiles was 1.102 g. A good correlation was then found between the performed experiments and the theory applied according to [42].

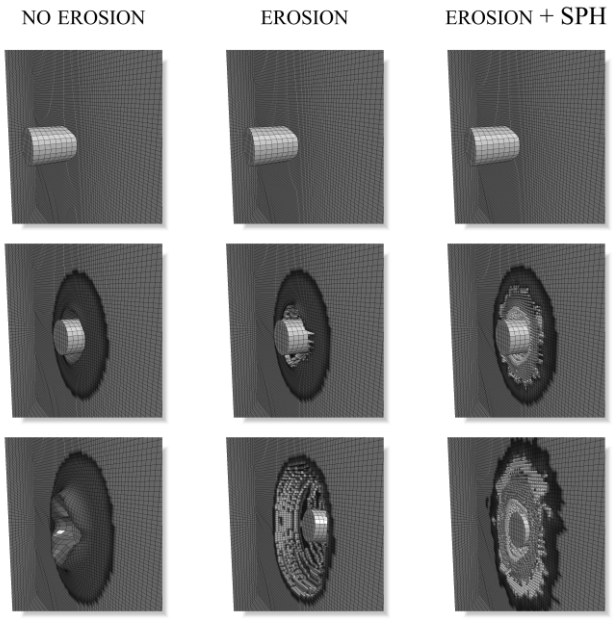

Fig. 5. Phases of the penetration of a concrete block. From the left: model variant with no erosion, with erosion and with erosion and adaptive transformations into SPH.

The results of the numerical simulation of the experiment are presented in graphical form in Fig. 5. The image shows the stages of penetration of a projectile with an impact speed of 500 ms^{-1}. Once again, on the left, there is the numerical model without element erosion, in the middle there is the model with erosion and on the right there is the model which also contained the transformation of eroded elements into SPH particles. The size of the crater in the final stage of penetration (i.e. the quantity of eroded elements) increased exponentially with the growing impact speed of the projectile. This was echoed by the considerably greater depth of penetration for model with erosion in contrast with the model without erosion and the model with SPH particles.

However, this is not in accordance with the experiment. The area of the measured data is marked in gray in Fig. 6. At higher speeds it is thus unacceptable to choose the permitted numerical erosion function without further investigation with regard to the fact that the penetration depth increases excessively with increasing projectile impact speed.

The model without the erosion of elements approximates the measured data well. However, due to the large degree to which the elements deform, and the very small time steps resulting from this, the time required for the calculations grew uncontrollably.

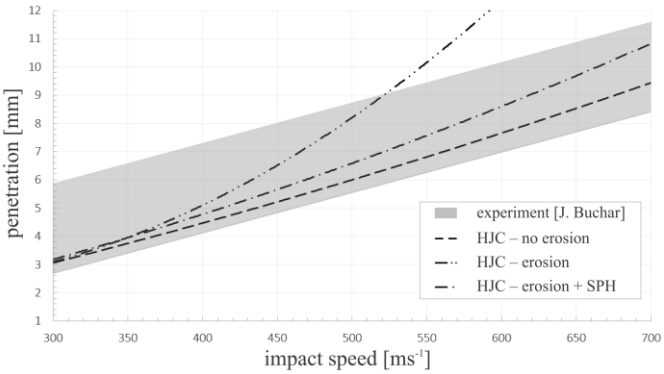

Fig. 6. Results of the experiment in comparison with numerical simulations.

The model in which the elements can transform into SPH particles also approximates the measured data well. Thanks to the erosion, it eliminates deformed elements and additionally provides a great deal of information about the behaviour of fragmenting particles of the model.

The SPH particles are present in the computational model right from the beginning of the simulation – they are inside the FEM elements, but inactive. The activation of the particles takes place at the moment when the erosion of the element commences, that is at $D_s < 0$.

Fig. 7 shows the stages of penetration by a projectile with an impact speed of 500 ms^{-1}. The picture also shows the gradual activation of the SPH particles. The interaction between the SPH particles and the still non-eroded elements is mediated by SPH particles inside the elements which are on the outer surface [1]. The number of active particles during the simulation with the projectile impact speed of 500 ms^{-1} is shown in Fig. 8.

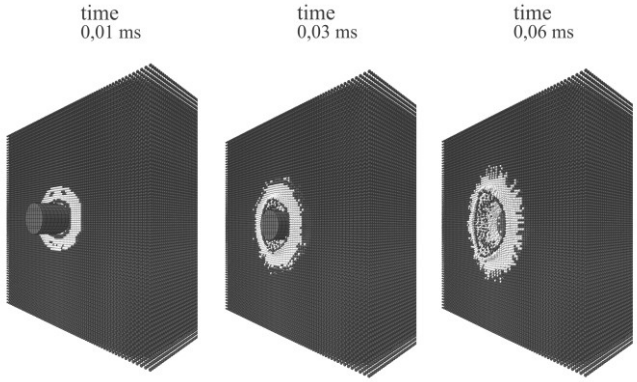

Fig. 7. Phases of the activation of SPH. Dark gray – inactive particles, white – active particles. Speed of the projectile: 500 ms^{-1}.

V. Conclusion

The contribution describes a simple experiment from the scientific field of terminal ballistics. It lists possible negative aspects of numerical simulations and simultaneously proposes a solution to these problems which consists in the numerical erosion of FEM elements and the subsequent preservation of their matter in the form of its adaptive transformation into SPH particles.

The implementation of numerical erosion in simulations can provide a useful tool for the removal of excessively deformed elements which can not only cause the extreme prolongation of the calculation but also its undesired locking, known as element locking. As matter and internal energy can be lost simply by implementing this numerical erosion, which can lead to the production of incorrect results, such dissipations have to be prevented. A suitable solution is therefore to use the adaptive transformation of eroded elements into SPH particles. These new particles assume the properties of elements which have eroded and subsequently create a certain residual strength due to their interaction with the surroundings, but in the sense of already damaged (i.e. loose) material.

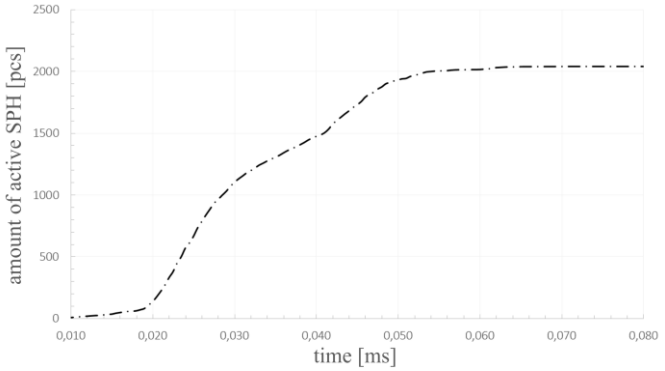

Fig. 8. Amount of active SPH particles through the simulation. Speed of the projectile: 500 ms^{-1}.

Acknowledgment

This outcome has been achieved with the financial support of project No. LO1408 "AdMaS UP - Advanced Materials, Structures and Technologies", supported by Ministry of Education, Youth and Sports under the „National Sustainability Programme I".

References

[1] LS-DYNA Keyword User's Manual, Volume II, 11/30/14 (r: 5876), Livemore Software Technology Corporation, Nov. 2014.

[2] P. Král, J. Kala, and P. Hradil, "Validation of the response of concrete nonlinear material models subjected to dynamic loading," in *Proceedings of the 9th International Conference on Continuum Mechanics*, Rome, Nov. 2015, pp. 182–185.

[3] P. Hradil, and J. Kala, "Analysis of the shear failure of a reinforced concrete wall," *Applied Mechanics and Materials*, vol. 621, pp. 124–129, 2014.

[4] P. Hradil, and J. Kala, "Nonlinear behaviour of the concrete specimen under shear load," in *Proceedings of 3rd International Conference on Mathematical, Computational and Statistical Sciences*, Dubai, Feb. 2015, pp. 248–253.

[5] J. Kala, and M. Hušek, "Useful material models of concrete when high speed penetrating fragments are involved," in *Proceedings of the 9th International Conference on Continuum Mechanics*, Rome, Nov. 2015, pp. 190–194.

[6] H-G. Kwak, and H. G. Gang, "An improved criterion to minimize FE mesh-dependency in concrete structures under high strain rate conditions," *International Journal of Impact Engineering*, vol. 86, pp. 84–95, 2015.

[7] J. Králik, "Safety of nuclear power plants against the aircraft attack," *Applied Mechanics and Materials*, vol. 617, pp. 76–80, August 2014.

[8] J. Králik, and M. Baran, "Numerical analysis of the exterior explosion effects on the buildings with barriers," *Applied Mechanics and Materials*, vol. 390, pp. 230–234, August 2013.

[9] P. Hradil, J. Kala, and V. Salajka, "Analysis of roadside safety barrier using numerical model, safety and reliability: Methodology and applications," in *Proceedings of the European Safety and Reliability Conference*, ESREL 2014, pp. 29–32.

[10] P. H. Bischoff, and S. H. Perry, "Compressive behaviour of concrete at high strain rates," *Materials and Structures*, vol. 24, pp. 425–450, 1991.

[11] G. Cusatis, "Strain-rate effects on concrete behaviour," *International Journal of Impact Engineering*, vol. 38, pp. 162–170, April 2011.

[12] AUTODYN Theory Manual, Revision 4.3, Century Dynamics, November 2005.

[13] T. J. Holmquist, G. R. Johnson, and W. H. Cook, "A computational constitutive model for concrete subjected to large strains, high strain rates, and high pressures," in *Proceedings of the 14th International Symposium on Ballistics*, Quebec, 1993, pp. 591–600.

[14] G. R. Johnson, and T. J. Holmquist, "A computational constitutive model for brittle materials subjected to large strains, high strain rates and high pressures," in *Shock-wave and High Strain-rate Phenomena in Materials*, New York, 1992, pp. 1075–1082.

[15] H. Fenglei, W. Haijun, J. Qiankun, and Z. Qingming, "A numerical simulation on the perforation of reinforced concrete targets," *International Journal of Impact Engineering*, vol. 32, pp. 173–187, 2005.

[16] U. Nyström, and K. Gylltoft, "Comparative numerical studies of projectile impacts on plain and steel-fibre reinforced concrete, *International Journal of Impact Engineering*, vol. 38, pp. 95–105, 2011.

[17] I. M. Kamal, and E. M. Eltehewy, "Projectile penetration of reinforced concrete blocks: Test and analysis," *Theoretical and Applied Fracture Mechanics*, vol. 60, pp. 31–37, 2012.

[18] T. B. N. Melo, and M. V. Donadon, "Damage modeling in reinforced concrete shelters subjected to ballistic impact," *International Journal of Research in Aeronautical and Mechanical Engineering*, vol. 2, pp. 38–52, 2014.

[19] D. Yongxiang, and F. Shunshan, "Numerical simulation of flat-nose projectile penetrating concrete and soil target," in *3rd WSEAS International Conference on Applied and Theoretical Mechanics*, Spain, 2007.

[20] B. Luccionia, and G. Aráoz, "Erosion criteria for frictional materials under blast load," in *Mecánica Computacional*, Rosario, Argentina, 2011, pp. 1809–1831.

[21] Q. M. Li, S. R. Reid, and A. M. Ahmad-Zaidi, "Critical impact energies for scabbing and perforation of concrete target," *Nuclear Engineering and Design*, vol. 236, pp. 1140–1148, 2006.

[22] H. M. Wen, and Y. X. Xian, "A unified approach for concrete impact," *International Journal of Impact Engineering*, vol. 77, pp. 84–96, 2015.

[23] J. C. Bruhl, A. H. Varma, and W. H. Johnson, "Design of composite SC walls to prevent perforation from missile impact," *International Journal of Impact Engineering*, vol. 75, pp. 75–87, 2015.

[24] J. Králik, "Optimal design of NPP containment protection against fuel container drop," *Advanced Materials Research*, vol. 688, pp. 213–221, May 2013.

[25] J. Kala, P. Hradil, and M. Bajer, "Reinforced concrete wall under shear load – Experimental and nonlinear simulation," *International Journal of Mechanics*, vol. 9, pp. 206–212, 2015.

[26] Z. Kala, "Sensitivity and reliability analyses of lateral-torsional buckling resistance of steel beams," *Archives of Civil and Mechanical Engineering*, vol. 15, no. 4, pp. 1098–1107, 2015.

[27] Z. Kala, J. Kala, M. Škaloud, and B. Teplý, "Sensitivity analysis of the effect of initial imperfections on the (i) ultimate load and (ii) fatigue behaviour of steel plate girders," *Journal of Civil Engineering and Management*, vol. 11, no. 2, pp. 99–107, 2005.

[28] F. Hokeš, J. Kala, and O. Krňávek, "Optimization as a tool for the inverse identification of parameters of nonlinear material models," in *Proceedings of the 9th International Conference on Continuum Mechanics*, Rome, Nov. 2015, pp. 50–55.

[29] F. Fedorik, J. Kala, A. Haapala, and M. Malaska, "Use of design optimization techniques in solving typical structural engineering related design optimization problems," *Structural Engineering and Mechanics*, vol. 55, no. 6, pp. 1121–1137, Sep. 2015.
[30] I. Kojima, "An experimental study on local behavior of reinforced concrete slabs to missile impact," *Nuclear Engineering and Design*, vol. 130, pp. 121–132, 1991.
[31] R. Ranjan, S. Banerjee, R. K. Singh, and P. Banerji, "Local impact effects on concrete target due to missile: An empirical and numerical approach", *Annals of Nuclear Energy*, vol. 68, pp. 262–275, 2014.
[32] C. Y. Tham, "Numerical and empirical approach in predicting the penetration of a concrete target by an ogive-nosed projectile," *Finite Elements in Analysis and Design*, vol. 42, pp. 1258–1268, 2006.
[33] J. A. Sherburn, M. J. Roth, J. S. Chen, and H. Hillman, "Meshfree modeling of concrete slab perforation using a reproducing kernel particle impact and penetration formulation," *International Journal of Impact Engineering*, vol. 86, pp. 96–110, 2015.
[34] R. Vignjevic, J. Campbell, and L. Libersky, "A treatment of zero-energy modes in the smoothed particle hydrodynamics method," *Comput. Methods Appl. Mech. Engrg.*, vol. 184, pp. 67–85, 2000.
[35] G. R. Johnson, "Artificial viscosity effects for SPH impact computations," *Int. J. Impact Engng.*, vol. 18, no. 5, pp. 477–488, 1996.
[36] J. J. Monaghan, "Smoothed particle hydrodynamics," *Annu. Rev. Astron. Astrophys.*, vol. 30, pp. 543–574, 1992.
[37] K-C. Wu, B. Li, and K-C. Tsai, "The effects of explosive mass ratio on residual compressive capacity of contact blast damaged composite columns," *Journal of Constructional Steel Research*, vol. 67, pp. 602–612, 2011.
[38] J. Zukas, "Introduction to hydrocodes," *Studies in applied mechanics*, Elsevier, vol. 49, 2004.
[39] Z. L. Wang, J. G. Wang, and W. J. Yang, "A simple numerical scheme for evaluating impact-induced compression damage in concrete plate," *Magazine of Concrete Research*, vol. 11, pp. 795–801, 2010.
[40] G. R. Liu, and M. B. Liu, *Smoothed particle hydrodynamics: a meshfree particle method*, New Jersey: World Scientific, 2003, 449 p., ISBN 981-238-456-1.
[41] J. Buchar, J. Voldřich, S. Rolc, and M. Lazar, "Response of concrete to the impact of fragments simulating projectiles," in *20th International Symposium on Ballistics*, Orlando, FL, 2002, pp. 23–27.
[42] M. J. Forrestal, B. S. Altman, J. D. Cargille, and S. J. Hanchack, "An empirical equation for penetration depth of ogive-nose projectile into concrete targets," *Int. J. Impact Engng*, vol. 15, pp. 395–405, 1994.